CHROMATICITY INVESTIGATION OF CURCUMINOID DYE COMPOSITE FOR WHITE LIGHT DOWN-CONVERSION

MAHMOOD SHAIKHAN TA'EEB AL SHAFOURI

UNIVERSITI SAINS MALAYSIA

2020

CHROMATICITY INVESTIGATION OF CURCUMINOID DYE COMPOSITE FOR WHITE LIGHT DOWN-CONVERSION

by

MAHMOOD SHAIKHAN TA'EEB AL SHAFOURI

Thesis submitted in fulfilment of the requirements
for the degree of
Doctor of Philosophy

December 2020

ACKNOWLEDGEMENT

In the name of Allah, Most Gracious, Most Merciful

First and foremost, I would like to express my gratitude to Allah Almighty for his mercy and bounty for giving me health and patience to complete this PhD study. I owe my gratitude to my main supervisor Dr. Naser Mahmoud Ahmed, for motivation, guidance and support throughout my program. I have been really blessed to have such supervisor who was very much interested about my project, and who always reacted to my inquiries and requests so quickly, I utmost gratitude to him. My gratitude and appreciation also goes to my co-supervisor Prof. Dr. Zainuriah Hassan, for her support, concern and assistance in ensuring the completion of my research. My gratitude also goes to my field supervisor Dr. Munirah Abdullah Al-Messiere for her cooperation and support throughout my program.

I am also very grateful to Universiti Sains Malaysia for providing the appropriate environment to complete my research. My gratitude also goes to the staff of School of Physics, NOR lab and solid state lab for their standing assistance. My appreciation and gratitude to all my friends and colleagues, thank you for your assistance and support.

Lastly, but not least, I express my appreciate to my parents , wife, kids, brothers and sisters for their continual support and prayers. I am forever grateful for their patience, concern, care, love and moral support.

Mahmood Al Shafouri

USM, Malaysia 2020

TABLE OF CONTENTS

ACKNOWLEDGEMENT ..... **ii**

TABLE OF CONTENTS ..... **iii**

LIST OF TABLES ..... **vii**

LIST OF FIGURES ..... **viii**

LIST OF SYMBOLS ..... **xiii**

LIST OF ABBREVIATIONS ..... **xv**

ABSTRAK ..... **xviii**

ABSTRACT ..... **xxi**

CHAPTER 1 INTRODUCTION **1**

1.1 Introduction 1

1.2 Problem statement 4

1.3 Scope of study 5

1.4 Objective of this study 5

1.5 Originality of this research 6

1.6 Outline of the thesis 6

CHAPTER 2 LITERATURE REVIEW **8**

2.1 Introduction 8

2.2 Solid-state lighting 8

2.3 White Organic LEDs 12

2.4 Concepts of light down-conversion 14

2.5 Organic dyes 15

2.5.1 Band gap of organic materials 16

2.5.2 Electronic Excitation in Organic Molecules 18

2.5.3 Types of absorbing electrons 19

2.5.4 Tauc method for optical absorption edge determination 22

2.6 Turmeric (Curcuma longa L.) 24
2.7 Extracting curcuminoid dye from Curcuma 26
2.8 Fluorescent layer preparation 27
2.8.1 Material and polymer composite technique 27
2.8.2 Electrospinning 30
2.9 Definition of lighting terms 34
2.10 Stress test 37
CHAPTER 3 METHODOLOGY AND INSTRUMENTATION 38
3.1 Introduction 38
3.2 White light generated by remote phosphor using curcuminoid dye 40
3.2.1 Extracting methods for curcuminoid dye 40
3.2.1(a) Hotplate extraction of curcuminoid dye 40
3.2.1(b) Extracting curcuminoid dye using the Soxhlet apparatus 41
3.2.1(c) Extracting curcuminoid dye by combination method 42
3.2.2 Sample preparation 42
3.2.3 Colorimeter measurement setup 47
3.3 White light generated by curcuminoid nanofibers using electrospinning 48
3.3.1 Preparation of polymer PMMA 48
3.3.2 Extracting curcuminoid dye using a centrifuge 49
3.3.3 Cleaning of glass substrates 49
3.3.4 Electrospinning setup 50
3.3.5 Annealing processes 51
3.3.6 White light emission testing 51
3.4 Structural and morphological characterizations 53
3.4.1 XRD 53
3.4.2 FESEM 54
3.4.3 FTIR 55

3.5 Optical characterization 57
3.5.1 Optical absorption (UV-Vis) 57
3.5.2 Colorimeter 58
3.5.3 Stress test 60
3.6 Summary 60
CHAPTER 4 THE RESULTS OF PHOSPHOR PREPARED BY SILICONE RUBBER AND CURCUMINOID 61
4.1 Introduction 61
4.2 XRD measurement 61
4.3 FTIR analysis 62
4.4 Absorption 64
4.5 Down-conversion light using one type of pumping source 68
4.6 Down-conversion of light using different pumping sources 74
4.7 Stress testing using one source 79
4.8 Stress testing using different pumping sources 80
4.9 Yellow/blue ratio 83
4.10 Summary 85
CHAPTER 5 THE RESULTS OF PHOSPHOR PRODUCED BY ELECTROSPINNING TECHNIQUE 86
5.1 Introduction 86
5.2 FESEM image analyses 86
5.3 FTIR spectra 90
5.4 Absorption and transmittance spectra 94
5.5 Fluorescence spectra 98
5.6 Stress Testing 107
5.7 Summary 109
CHAPTER 6 CONCLUSION AND FUTURE RECOMMENDATIONS ... 111
6.1 Conclusion 111

6.2 Recommendations for future research.....112

REFERENCES.....114

LIST OF PUBLICATIONS

INTERNATIONAL CONFERENCES

LIST OF TABLES

Page

Table 2.1 Discoveries and History of LEDs (Khanna, 2014).....9

Table 2.2 Organic dyes used in down-conversion.....16

Table 2.3 Materials used in electrospinning for various purposes. 33

Table 4.1 Best results for the chromaticity coordinates (CIE) 74

Table 5.1 Band assignments of various functional groups obtained from FTIR spectral analyses.....91

Table 5.2 Comparison of the change of CIE coordinates with the change of annealing temperature (100 °C, 200 °C, and 300 °C) of as-prepared PICNF-5, PICNF-10 and PICNF-15 104

LIST OF FIGURES

Page

Figure 1.1 Structure of curcuminoids: curcumin, bis-demethoxycurcumin and demethoxycurcumin (Farooqui & Farooqui, 2019). 3

Figure 2.1 Schematics of p-n junction for LED 11

Figure 2.2 Main parts of conventional LED 11

Figure 2.3 Classic heterjunction OLED structure 12

Figure 2.4 Main steps of the production of white light using remote phosphor 14

Figure 2.5 Formation of HOMO and LUMO gap (Bredas, 2014). 18

Figure 2.6 Various electronic excitations that occur in organic molecules (Thejokalyani & Dhoble, 2014) 20

Figure 2.7 Simple absorption spectrum for molecules. 21

Figure 2.8 Example Tauc plot from the UV-vis analysis of Gamal (*Gliricidia Sepium*) leaves extract, that illustrates the method of fitting the linear region to evaluate the bandgap at the X axis intercept (approximately 1.83 eV) (Johannes et al., 2020). 24

Figure 2.9 Energy level between HOMO and LUMO of natural photosensitizer (curcumin) (Rahamathullah, Khairul, Ku Bulat, & Hussin, 2015). 25

Figure 2.10 Encapsulant methods: (A) phosphor layer is coated on the diode and (B) the phosphore or dye is mixed with epoxy. 28

Figure 2.11 Structure of silicone rubber (Polydimethylsiloxane (PDMS)) (Sperling, 2005). 29

Figure 2.12 Schematic of a typical setup for electrospinning (Nikmaram et al., 2017). 30

Figure 2.13 CIE standard observer color-matching functions (Rea & Freyssinier, 2010). 35

Figure 2.14 The CIE 1931 chromaticity diagram (Jaquet, 2007). 36

Figure 3.1 Flowchart of experimental steps.....39

Figure 3.2 Soxhlet apparatus setup 41

Figure 3.3 Mold processing samples.....43

Figure 3.4 Flowchart illustrating the steps of experimental method (M1). 44

Figure 3.5 Flowchart illustrating the steps of experimental method (M2). 45

Figure 3.6 Flowchart illustrating the steps of experimental method (M3). 46

Figure 3.7 Colorimeter measurement setup. 48

Figure 3.8 A. Schematic presentation of the electrospinning set up for PICNF synthesis and B. Image of the electrospinning device. 50

Figure 3.9 Flowchart illustrating the experimental stages of phosphor production using electrospinning.....52

Figure 3.10 (A.) Image of the HR-XRD and (B.) Schematic of X-ray diffraction. 54

Figure 3.11 Schematic of FESEM (Zhou & Wang, 2007).....55

Figure 3.12 Illustration of Fourier-transform infrared (FT-IR) spectrometer (Sundeep, Krishna, & Kumar, 2017). 56

Figure 3.13 Illustration of the inner components of the Cary Series 5000 UV-vis–NIR spectrophotometer. 58

Figure 3.14 Colorimeter apparatus.....59

Figure 3.15 Main screen of the parameters measured by the colorimeter. 59

Figure 4.1 XRD patterns (black line) for pure Curcuma powder, (red line) for silica gel (S.G) and (blue line) for phosphor Ph3. 62

Figure 4.2 FTIR analysis of phosphor Ph3 (black line), curcuma (red line), and silica gel (S.G) (blue line). 63

Figure 4.3 Absorption and Fluorescence for phosphor Ph3 weight 40mg and operated at 60 mA.....65

Figure 4.4 Absorption for three different phosphor (Ph1, Ph2, and Ph3) with different weights A. 20, B. 30, and C. 40 mg. 66

Figure 4.5 Absorption for different phosphor : (A) phosphor Ph1, (B) phosphor Ph2, and (C) phosphor Ph3 with different weights (10, 20, 30, 40, and 50 mg). 67

Figure 4.6 Electroluminescence spectra (EL) of phosphor Ph1, pumping wavelength (390nm) at I=60mA..... 69

Figure 4.7 Electroluminescence spectra (EL) of phosphor Ph2, pumping wavelength (390nm) at I=60mA..... 69

Figure 4.8 Electroluminescence spectra (EL) of phosphor Ph3, pumping wavelength (390nm) at I=60mA..... 70

Figure 4.9 CIE chromaticity coordinates for phosphor Ph1 at I=60mA..... 71

Figure 4.10 CIE chromaticity coordinates for phosphor Ph2 at I=60mA..... 71

Figure 4.11 CIE chromaticity coordinates for phosphor Ph3 at I=60mA..... 72

Figure 4.12 CIE chromaticity coordinates for phosphor Ph1, Ph2 and Ph3 at weight =35mg and wavelength pumping source 390nm. 73

Figure 4.13 CIE chromaticity coordinates (a) and Electroluminescence spectra (EL) (b) for Ph3 phosphor (10 mg) at I=20 mA pumped by wavelength (365, 390, and 445 nm). 76

Figure 4.14 CIE chromaticity coordinates (a) and electroluminescence spectra (EL) (b) for Ph3 phosphor (30 mg) at I=100 mA pumped by wavelength (365,390, and 445 nm). 77

Figure 4.15 CIE chromaticity coordinates (a) and Electroluminescence spectra (EL) (b) for Ph3 phosphor (50 mg) at I=20 mA pumped by wavelength (365, 390, and 445 nm). 78

Figure 4.16 Light coordination in CIE chromaticity diagram: A) phosphor sample on the LED source directly, B) with air gap (1.1 mm), and C) with air gap (2.2 mm). 80

Figure 4.17 Light Emitting Coordination in CIE chromaticity diagram during stress test comparison between three types of wavelength pumped (365,390 and 445nm) during 10 min. 82

Figure 4.18 (a) Structure of curcumin, and the degradation products reported in the literature: (b) trans-6-(40-hydroxy-30-methoxyphenyl)-2,4-dioxo-5-hexanal (enol form), and (c) vanillic acid (Canamares et al., 2006). 82

Figure 4.19 Planckian locus in the CIE 1931 chromaticity diagram (Khan, 2013). 84

Figure 4.20 The relationship between Y/B and CCT for three deferent concentrations Ph3 (25, 35 and 50mg) with three deferent currents (20, 60 and 100mA). 84

Figure 5.1 FESEM images of as-prepared PICNFs with varying PMMA contents of (A) 5 wt%, (B) 10 wt%, and (C) 15 wt%..... 87

Figure 5.2 FESEM images of as-prepared PICNF-15 88

Figure 5.3 FESEM images of PICNF-15 (A) without annealing and annealed at (B) 100 ^{o}C, (C) 200 ^{o}C, (D) 300 ^{o}C and (E) nanoparticles diameter (annealed 300 ^{o}C) 89

Figure 5.4 Cross-section of (A) as-prepared and (B) post-annealed nanofibers at 200 °C 90

Figure 5.5 FTIR spectra of PMMA-15 nanofibers. 92

Figure 5.6 FTIR spectra of pure curcuma. 92

Figure 5.7 FTIR spectra of as-prepared PICNF-15..... 93

Figure 5.8 FTIR spectra of post-annealing PICNF-15 (200 ^{o}C). 93

Figure 5.9 Absorption spectra of PMMA-15 Nanofibers, as-prepared PICNF-15 and post-annealed PICNF-15. 95

Figure 5.10 Light transmittance curves of PMMA-15 Nanofibers, as-prepared PICNF-15 and post-annealed PICNF-15. 96

Figure 5.11 Tauc plot for as-prepared PICNF-15 and post-annealed PICNF-15. 97

Figure 5.12 Comparative evaluation of absorption and fluorescence spectra of as-prepared PICNF-15 and post-annealed PICNF-15. 97

Figure 5.13 Curcuminoid solution volumes (1, 3, and 5 ml) dependent EL spectra (A) and CIE plot of as-prepared PICNF-5 (B). Inset tables show the corresponding Y/B and white light CIE co-ordinates. 99

Figure 5.14 The EL spectra (A) and CIE plot (B) (excitation wavelengths of 365, 390 and 445 nm from LED) of as-prepared PICNF-5. Inset tables show the corresponding Y/B and white light CIE co-ordinates.....102

Figure 5.15 The EL spectra (A) and CIE plots (B) of PICNF-5, PICNF-10 and PICNF-15 obtained at 445 nm (100 mA) excitation by using 3 ml of curcuminoid solution as a function of PMMA concentrations of 5, 10 and 15 wt% . Inset tables show the corresponding Y/B and white light CIE co-ordinates. 103

Figure 5.16 Comparison of the change of CIE chromaticity coordinates with the change of annealing temperature (100 °C, 200 °C, and 300 °C) of as-prepared (A.) PICNF-5, (B.) PICNF-10 and (C.) PICNF-15 samples containing 1 ml of curcuminoid solution pumped by the LED wavelength of 365 nm at a current of 100 mA. 105

Figure 5.17 Changing current (20, 60, and 100 mA) dependent variation in the CIE chromaticity coordinates values of PICNF-5 containing 1 ml of curcuminoid solution pumped by LED wavelength of 365 nm. Inset tables show the corresponding CIE co-ordinates.....106

Figure 5.18 Light emitting coordinates in the CIE chromaticity diagram of PICNF-15 (Pre-annealed) recorded for 30 minutes pumped by the light sources wave (A) 365nm, (B) 390nm and (C) 445 nm. Inset tables show the corresponding CIE co-ordinates. 108

Figure 5.19 Light emitting coordinates in the CIE chromaticity diagram of PICNF-15 (post-annealed) pumped by the light sources wave 365, 390, and 445 nm. Inset tables show the corresponding CIE co-ordinates.....109

LIST OF SYMBOLS

Å	Angstrom
A	Proportionality constant
c	Speed of light
D	Average crystallite size
$d_{h\,k\,l}$	Inter-plane distance between the two neighboring lattice planes
E	Energy
E_g	Band gap
eV	Electron volt
g	Gram
G	Gauge
h	Planck's constant
hν	Energy of photon
I	Current
I	Emitted radiation intensity
K	Kelvin
k	Boltzmann's constant
n	Nature of the electronic transition
n	Integer order
^{o}C	Celsius
OH	Hydroxyl
T	Temperature
T	Blackbody temperature
V	Volt
v	Frequency of light
W	Watt

X	X-axis
Y	Y-axis
α	Absorption coefficient
β	Full width at half maximum
θ	Bragg's angle
λ	Wavelength
π	Pi
σ	Sigma

LIST OF ABBREVIATIONS

Abs	Absorbance
AC	Alternating current
AlGaInP	Aluminium gallium indium phosphide
a.u.	Arbitrary unit
BDMC	Bis-demethoxycurcumin
Bio-HLEDs	Bio hybrid light emitting diodes
BODIPY	Boron-dipyrromethene
BT	2,1,3-benzothiadiazole
CIE	Chromaticity coordinates
CCT	Correlated color temperature
CRI	Color rendering index
CUR	Curcumin
DMC	Demethoxycurcumin
DMF	Dimethylformamide
DNA	Deoxyribonucleic acid
EDX	Energy dispersive
EL	Electroluminescence
EML	Emissive layer
ESIPT	Excited state intramolecular proton transfer
ETL	Electron-transporting layer
FESEM	Field emission scanning electron microscope
Fig.	Figure
FTIR	Fourier-transform infrared spectroscopy
FWHM	Full width at half maximum
GaAs	Gallium arsenide
GaN	Gallium nitride
GaP	Gallium phosphide
GaSb	Gallium antimonide
HOMO	Highest occupied molecular orbital
HTL	Hole-transporting layer
InGaN	Indium gallium nitride

InP	Indium phosphide
IR	Infrared
ITO	Indium tin oxide
LED	Light-emitting diode
LUMO	Lowest unoccupied molecular orbital
M1	Method 1
M2	Method 2
M3	Method 3
MEH-PPV	poly[2-methoxy-5-(2′-ethyl-hexyloxy)1,4-phenylene-vinylene]
NIR	Near-infrared
n-type	Negative type
OLED	Organic light emitting diode
PDMS	Polydimethylsiloxane
PEO	Polyethylene oxide
PICNFs	Poly(methyl methacrylate) integrated curcuminoid nanofibers
PMMA	Poly(methyl methacrylate)
p-n	Positive-Negative
Pom	Pomegranate
p-type	Positive type
PVC	Poly(vinyl chloride)
Ra	Rending index
RCA	Radio Corporation of America
RE	Rare Earth
RT	Room temperature
S.G	Silica gel
SiC	Silicon carbide
SSL	Solid state light
T	Transmittance
TPA-Flu	Triphenylamine with fluorene
Tur	Turmeric
UV	Ultra-violet
UV-Vis	Ultraviolet-visible
WLED	White light emitting diode
XRD	X-ray diffraction

Y/B	Yellow per Blue
YAG	Yttrium Aluminium Garnet
ZnO	Zinc oxide

KAJIAN KROMATIK KOMPOSIT PEWARNA KURKUMINOID UNTUK PENUKAR-TURUN CAHAYA PUTIH

ABSTRAK

Sasaran utama kajian kerja yang dibentangkan dalam thesis ini adalah untuk menghasilkan cahaya putih menggunakan pewarna curcuminoid dengan kaedah yang mudah dan jimat : fosfor curcuminoid dengan getah silikon dan Poli (metil metakrilat) gentian nanofiber curcuminoid bersepadu (PICNFs). Dalam proses mencapai sasaran utama, kaedah yang paling berkesan perlu dikaji dengan teliti untuk mengekstrak pewarna curcuminoid daripada Curcuma serta menentukan parameter PMMA yang optimum untuk penyediaan gentian nanofiber curcuminoid. Kajian ini juga bertujuan untuk membandingkan dan meningkatkan jangka hayat cahaya putih dengan mengurangkan degradasi pewarna curcuminoid dengan beberapa cara, seperti menggunakan jurang antara sumber cahaya dan lapisan fosfor atau dengan menyepuhlindapan gentian nanofiber. Curcuminoids diekstrak dari (Curcuma longa L.) dan digunakan sebagai pewarna organik untuk penghasilan cahaya putih melalui penukaran panjang gelombang. Pewarna yang diekstrak daripada Curcuminiod dirawat menggunakan dua jenis kaedah : kaedah yang pertama adalah dengan mencampurkan pewarna dengan gel silika untuk menghasilkan fosfor dan seterusnya mencampurkanya dengan getah silikon untuk menghasilkan cakera yang merangkumi sumber diod pemancar cahaya biru (LED biru) dan LED ultraviolet (UV-LED), kaedah yang kedua pula adalah dengan mencampurkan Curcuma dengan polimer (metil metakrilat) polimer (PMMA) untuk menghasilkan gentian nanofiber dan nanopartikel curcuminoid melalui proses elektrospin.Dalam pendekatan kaedah yang pertama, curcuminoid diekstraksi dari Curcuma melalui tiga kaedah kecil: kaedah hotplate

(M1), penggunaan alat Soxhlet (M2), dan gabungan kedua-duanya (M3).Tekstur melekit curcuminoid diatasi dengan mencampurkan larutan curcuminoid dengan silika gel. Serbuk yang dihasilkan setelah campuran kering, disebut curcuminoid fosfor Ph, iaitu serbuk yang dicampurkan dengan silikon getah. Sampel yang dihasilkan dipam dengan tiga panjang gelombang LED yang berbeza (365, 390, dan 445 nm) untuk mendapatkan LED putih (WLED). Koordinat kromatik cahaya putih (CIE) dikawal dengan mengubah sumber pam LED, arus terpakai (20, 60, dan 100 mA) dan berat (10 hingga 50 mg) (kepekatan fosfor curcuminoid). Ujian tekanan juga dilakukan pada sampel untuk meningkatkan jangka hayat fosfor. Dalam kaedah pendekatan yang kedua, serbuk Curcuma dicampurkan dengan PMMA untuk menghasilkan gentian nano curcuminoid pada permukaan kaca melalui proses elektrospin. PMMA di bahagi dalam tiga tahap kepekatan iaitu berat sebanyak(5, 10, dan 15%)dan seterusnya dicampurkan dengan serbuk (curcuma longa L.) untuk menghasilkan larutan curcuminoid. Empar digunakan untuk memisahkan larutan curcuminoid dari kekotoran. Jumlah larutan polimer yang berbeza dicampur dengan curcuminoid (1 ml hingga 5 ml) dan elektrospun adalah kaedah untuk mengkaji sifatnya. Gentian nano yang dihasilkan diletakkan pada LED (365, 390, dan 445 nm) untuk mengawal fosfor yang dihasilkan . Kesan penyepuhlindapan terhadap sampel dikaji. Kaedah aplikasi fosfor dengan getah silikon dan kaedah gentian nano berjaya menghasilkan cahaya putih dengan nilai CIE masing-masing 0.33; 0.32 dan 0.302; 0.338. Berkaitan dengan kepekatan fosfor, kaedah gabungan M3 paling berkesan. Gentian nano curcuminoid terbentuk dalam bentuk yang sekata pada kepekatan PMMA 15% berat. Nilai diameter gentian nano curcuminoid adalah diantara 250 dan 300 nm. Selepas proses penyepuhlindapan, diameter nanopartikel yang purata ialah 9~18 nm. Melalui ujian tekanan, dihuraikan bahawa proses penyepuhlindapan

nanofiber berkesan untuk mengurangkan degradasi fosfor dan memperpanjangkan jangka hayatnya.

CHROMATICITY INVESTIGATION OF CURCUMINOID DYE COMPOSITE FOR WHITE LIGHT DOWN-CONVERSION

ABSTRACT

The main aim of the research work presented in this thesis was to produce white light using curcuminoid dye by simple and economical methods: curcuminoid phosphor with silicon rubber and Polymethyl methacrylate integrated curcuminoid nanofibers (PICNFs). To achieve this, it was necessary to study the most efficient way to extract curcuminoid dye from Curcuma and determine the optimum PMMA parameters for the preparation of curcuminoid nanofibers. This study also aimed to compare and improve the lifetime of white light by mitigating the degradation of curcuminoid dye in several ways, such as using a gap between the light source and phosphor layer or by annealing the nanofibers. Curcuminoids were extracted from *Curcuma longa L.* and used as an organic dye for the production of white light through wavelength down-conversion. The extracted dye was treated using two ways: first is to mix the dye with silica gel to produce phosphor then mix with silicone rubber to produce a disk that covers the blue light-emitting diode source (blue LED) and ultraviolet LED (UV-LED), and the second is to mix the Curcuma with polymethyl methacrylate polymer (PMMA) to produce curcuminoid nanofibers and nanoparticles through electrospinning. In the first approach, curcuminoid was extracted from Curcuma via three sub methods: hotplate method (M1), use of Soxhlet apparatus (M2), and combination of the first two (M3). The stickiness of curcuminoid was resolved by mixing the curcuminoid solution with silica gel. The powder produced after the mixture has dried is called curcuminoid phosphor Ph, which is mixed with silicone rubber. The resulting samples were pumped with three different LED wavelengths

(365, 390, and 445 nm) to obtain the white LED (WLED). White light chromaticity coordinates (CIE) was controlled by changing the LED pumping source, applied currents (20, 60, and 100 mA) and weights (10 to 50 mg) (concentration of the curcuminoid phosphor). A stress test was also performed on the samples to improve phosphor lifetime. In the second approach, Curcuma powder is mixed with PMMA to produce curcuminoid nanofibers on the glass through electrospinning. PMMA in three concentration levels (5, 10, and 15 wt%) was mixed with *(curcuma longa L.)* powder to produce a curcuminoid solution. A centrifuge was used to separate the curcuminoid solution from impurities. Different amounts of polymer solution mixed with curcuminoid (1 ml to 5 ml) were electrospun to study their properties. The resulting nanofibers are placed on the LED (365, 390, and 445 nm) as a remote phosphor. The effect of annealing on samples was also studied. The phosphor with silicone rubber and nanofibers produced white light with the CIE values of 0.33;0.32 and 0.302;0.338, respectively. With regards to phosphor concentration, the combination method, M3, is the most effective. The curcuminoid nanofibers formed uniform shape at PMMA concentration of 15 wt% . The diameter of curcuminoid nanofibers values was between 250 and 300 nm. After annealing, the average nanoparticle diameter was between 9 and 18 nm. Through stress testing, it was found that the annealing process of the nanofiber is effective to reduce phosphor degradation and extend its lifetime.

CHAPTER 1

INTRODUCTION

1.1 Introduction

Since 1994 have witnessed a significant development in the production of white light using light-emitting diode (LED) in preference to conventional light sources, such as fluorescent and incandescent lamps that are energy consuming and negatively impacts the environment. Compared with traditional lamps, LEDs have lower energy consumption, longer lifetime, and wider applications in indicators, lasers, displays, and fluorescent bio-medical tools (V. Singh & Mishra, 2015). Photophysical principles, such as hydrogen-bonding-mediated J-aggregation (Molla & Ghosh, 2012), fluorescence resonance energy transfer (Sanju, Neelakandan, & Ramaiah, 2011), excited state intramolecular proton transfer (S. Park et al., 2009), combined monomer and excimer fluorescence (Y. Liu, Nishiura, Wang, & Hou, 2006), and inter- and intra-molecular charge transfer (Y. Park et al., 2015), have been used to obtain white light emission that contains the three essential red, green, and blue components. Light down-conversion is currently one of the most important LED lighting technologies. In this process, high-energy (shorter wavelength) light from a LED is absorbed by a phosphorescent material and then re-emitted as a low-level energy (longer wavelength) light. The phosphorescent material is usually pumped with a blue light to ensure that it re-emits a green or red light and the resulting recombined light is white. Some organic dyes exhibit this phosphorescent behavior. Dyes are organic chemicals that are able to absorb and reflect light at selective wavelengths within the visible field of the electromagnetic spectrum (Hatch, 1993). The dyes that have or have been treated to behave like phosphorescent materials are called phosphor.

A high level of interest has been focused in the search for organic and inorganic molecules and materials that emit white light when photoexcited at near UV and blue wavelengths. Organic materials is preferable to inorganic ones due their low toxicity, low cost, and ease of fine-tuning (Mukherjee & Thilagar, 2014). Many researchers using organic materials obtained results close to the ideal light. Example of these materials are Lumogen® (Mosca et al., 2013) and BODIPY (Taylor-Shaw et al., 2016). A few studies applied dyes extracted from nature. Easily extracted and strongly fluorescent pigments can be found in many plants, one of which is (*Curcuma longa L.*), a widely known versatile species that is rich in dye.

Curcuma is a polyphenol and a member of the ginger plant family (Zingiberaceae) that frequently appears in yellow color and is exploited as a spice and color agent (Chattopadhyay, Biswas, Bandyopadhyay, & Banerjee, 2004; Patra & Barakat, 2011).This plant has been incorporated into systems of traditional medicine to treat several diseases due to its antibacterial, cardioprotective, antidiabetic, radioprotective, antimutagenic, and hepatoprotective effects (Cunha Neto, Marton, de Marqui, Lima, & Barbalho, 2018; Dutta, 2015). The main components extracted from Curcuma are curcuminoids, namely, curcumin (curcumin I) (CUR), demethoxycurcumin (curcumin II) (DMC), and bis-demethoxycurcumin (curcumin III) (BDMC) (Aggarwal et al., 2006; Hatamipour, Sahebkar, Alavizadeh, Dorri, & Jaafari, 2019; Itaya et al., 2019). Fig. 1.1 shows the structure of the three types of curcuminoids (Farooqui & Farooqui, 2019).

In light down-conversion, the phosphorescent materials are composited with polymers and used as a remote phosphor. Polymers are long-chain molecules with high molecular weight often measured in hundreds of thousands. The viscosity of the members increases with the molecular weight of the series (Sperling, 2005).

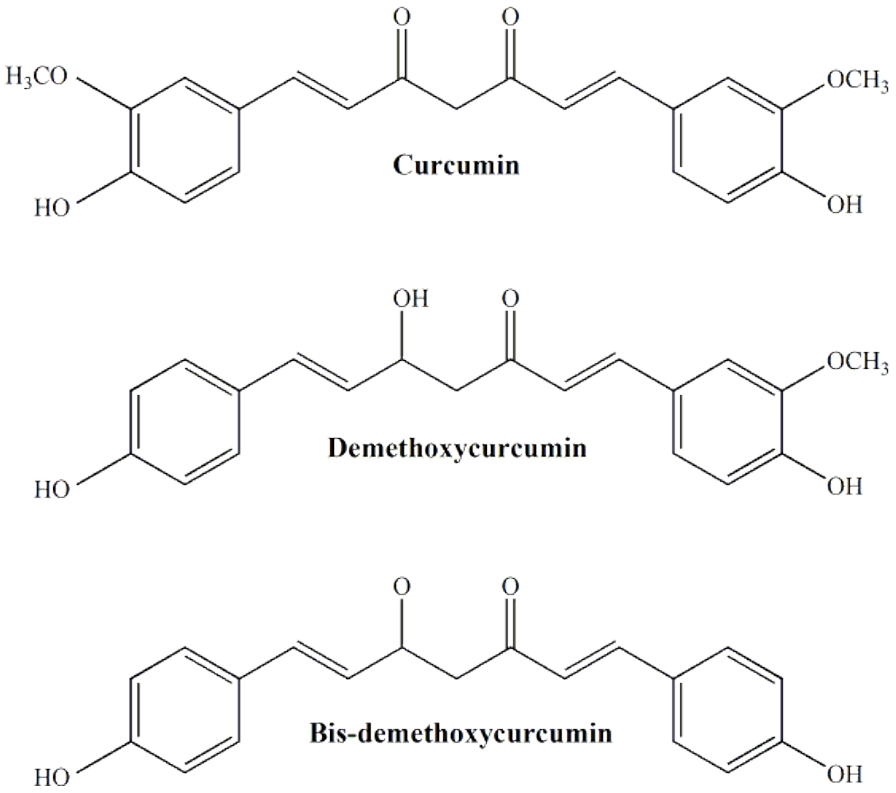

Figure 1.1 Structure of curcuminoids: curcumin, bis-demethoxycurcumin and demethoxycurcumin (Farooqui & Farooqui, 2019).

Synthetic and natural polymers play an essential and ubiquitous role in everyday life because of their broad range of properties and several characteristics, such as chemical stability, light weight, elasticity, availability of raw materials for large production, and easy and flexible processing methods (Lu, Shah, & Xu, 2017). Polymers have many types, including poly(methyl methacrylate) (PMMA), poly(vinyl chloride), silicone, and hydroxy acrylates; dissolve in different types of solvents, such as water, dimethylacetamide, methylethyl ketone, acetone, and ethyl acetate; and have unique characteristics and uses. For example, polybutene is used for films, and cellulose acetate butyrate is used for irrigation pipes (Ebewele, 2000). Phosphorescent materials can be mixed with polymers such as silicone rubber to produce a disc cover for LEDs or with PMMA to produce nanofibers through electrospinning.

Electrospinning is a simple and efficient technique to prepare polymeric nanofibers (Rüzgar, Birer, Tort, & Acartürk, 2013). The idea of an electrospinning

device began more than a century ago, specifically in 1902, and is based on Cooley pattern and Morton (Mirjalili & Zohoori, 2016). A wide array of possible formulations can be generated because most polymers can be electrospun (Rüzgar et al., 2013). The basic electrospinning components are a syringe pump, a syringe with nozzle, a conductive collector, and a high-voltage source (Macossay, Marruffo, Rincon, Eubanks, & Kuang, 2007; Mohammadian & Haghi, 2014; Shin, Purevdorj, Castano, Planell, & Kim, 2012). Owing to the electrostatic field between nozzle and collector, the polymer solution (nanofibers) is collected on the surface of the collector screen (Mirjalili & Zohoori, 2016). Many parameters, such as polymer molecular weight, solution viscosity, needle diameter, and distance between the needle and collector, can be tuned to generate fibers of various thicknesses (Lu et al., 2017).

1.2 Problem statement

White light is produced by several methods, and one of the most famous is called down-conversion wavelength that uses phosphor produced from organic or inorganic materials. Rare earth (RE) is the most common inorganic materials used in this technique. RE phosphors can divert the light from UV or blue to visible and/or near infrared. Yttrium aluminum garnet (YAG) is one of the most common phosphor host materials of RE ions (Almessiere et al., 2018). However, the RE materials are expensive, have a certain percentage of toxicity and require long preparation.

Organic dyes are a suitable alternative to inorganic dyes in this field, as many studies have obtained results close to ideal white light (Findlay et al., 2014). There are many natural sources of organic dyes that do not require complicated processes to produce dyes from them, but only a few studies used dyes extracted from nature (V.

Singh & Mishra, 2015). The reason may be due to the rapid degradation of natural dyes.

Through previous literature studies, there is only one study in which the dye extracted from Curcuma was used to produce white light, but the dye extracted from Pomegranate was used with it (V. Singh & Mishra, 2015), and this doubles the time and effort in the extraction processes.

Curcuminoid dye and nanocurcuminoid particles extracted from Curcuma can be a good alternative to inorganic materials because they are inexpensive, non-toxic, and easily extracted .

1.3 Scope of study

Two simple techniques were developed to produce white light using curcuminoid dye. The first method mixes the curcuminoid dye with silicone rubber to produce a disk covering the LED, and the second method combines the curcuminoid dye with PMMA to produce nanofibers and nanoparticles through electrospinning. Three different wavelength LEDs (365, 390, and 445 nm) were used to pump the samples. The structural and optical properties of samples were studied, and XRD, FESEM, FTIR, Abs%, EL, and CIE were measured.

1.4 Objective of this study

The main objectives of this study can be summarized in the following points:

1. To study the most efficient way to extract curcuminoid dye from Curcuma.
2. To study the effect of the light pumping source wavelength and current on the coordinates of light produced from phosphor.
3. To produce white light using curcuminoid dye.

4. To determine the optimum PMMA parameters for the preparation of curcuminoid nanofibers.

5. To compare and improve the lifetime of white light by mitigating the degradation of curcuminoid dye in several ways, such as using a gap between the light source and phosphor layer or by annealing the nanofibers.

1.5 Originality of this research

The originality of this study is based on the following points:

1- An innovative way to synthesize phosphor by mixing curcuminoid dye with silica gel.

2- White light is produced using curcuminoid dye for the first time.

3- In this work, nano-curcuminoid particles from curcuminoid nanofibers were fabricated, which was used to produce white light.

1.6 Outline of the thesis

This work consists of six chapters. Chapter 1 discusses general overview of the subject, problem statement, scope of study, thesis aim and objectives, and originality of the thesis. Chapter 2 provides the literature review and theoretical background of white LED, concepts of light down conversion, material and polymer composite technique, nanofiber and electrospinning technique, and curcuminoid pigment. Chapter 3 describes the methodology and the instrumentation used for material characterization. Chapter 4 presents the structural results and optical properties of curcuminoid extracted from Curcuma via three methods: hotplate method (M1), use of Soxhlet apparatus (M2), and combination of the first two (M3). Chapter 5 presents the structural results and optical properties of nanofiber curcuminoid synthesized

through electrospinning. Chapter 6 presents the conclusions and suggestions for future works.

CHAPTER 2

LITERATURE REVIEW

2.1 Introduction

The involved general principles and theories are presented. This chapter begins with a historical overview of the genesis and evolution of LED with a brief explanation of basic LED construction, followed by different approaches to generate white organic light with LEDs. Organic materials were discussed in terms of organic deys, optical bandgap, electronic excitation in organic molecules, and electron absorption mode. The main components of Curcuma (main material), the origin of its yellow color, the methods of extracting curcuminoid, the materials and techniques for polymer composite, and the method of electrospinning were reviewed.

2.2 Solid-state lighting

LED was first created in 1927 and the first commercial compound semiconductor. From a historical perspective (Table 2.1 (Khanna, 2014)), the British electrical engineer and experimenter Captain Henry (1881–1966) investigated the possibility of using carborundum or silicon carbide (SiC) crystals as rectifying solid-state detectors and called them “crystal detectors” in 1907. During his experiments on electric current flow through SiC, Round observed an interesting phenomenon: a yellowish light is emitted when a potential difference of ~10 V is applied across a SiC crystal. This finding marked the birth of the first LED. In 1962, Nick Holonyak Jr. of General Electric Copany first introduced an LED, particularly a red LED that emits light in the visible part of the frequency range.

Table 2.1 Discoveries and History of LEDs (Khanna, 2014)

No	Year	Event
1.	1907	The British scientist Captain Henry Joseph Round (June 2, 1881 to August 17, 1966), Marconi Labs, discovered electroluminescence using SiC crystal and a cat's whisker detector.
2.	1927	The Russian Oleg Vladimirovich Losev (May 10, 1903 to January 22,1942) independently reported the creation of LED in Russian, German, and British scientific journals but his research was ignored at that time.
3.	1955	Rubin Brunstein, Radio Corporation of America (RCA), USA, reported IR emission from GaAs and other semiconductor alloys such as GaSb, InP, and so on.
4.	1961	Robert Biard and Gary Pittman, Texas Instruments, USA, found that GaAs emitted IR on passing current and received patent for IR LED. Although the first LED, its emission was outside the spectrum of visible light.
5.	1962	First practical red LED developed by Nick Holonyak, Jr., General Electric Company; he is seen as the "father of the light-emitting diode."
6.	1968	Monsanto Company started mass-producing visible red LEDs using GaAsP.
7.	1972	M. George Crawford, former graduate student of Holonyak, invented yellow LED and raised the brightness of red and orange–red LEDs by a factor of 10.
8.	1972	First Blue LEDs were developed by Herbert Paul Maruska at RCA using gallium nitride (GaN) on a sapphire substrate.
9.	1976	Thomas P. Pearsall produced high-brightness, high-efficiency LEDs.
10.	1994	Replacement of GaAs substrate in AlGaInP red LED with transparent GaP.
11.	1994	First WLED. Shuji Nakamura, Nichia Corporation, Japan, demonstrated the first high-brightness blue LED based on InGaN; he is regarded as the inventor of the blue LED.
12.	1998	First commercial high-power LED.

The first blue LED was manufactured by Shuji Nakamura of Nichia Corporation in 1979 by using gallium nitride but only became low cost for commercial production in the 1990s (Khanna, 2014). The basic construction of an LED is a semiconductor p-n junction as shown in Fig. 2.1. The main parts of the conventional LED are seen in Fig. 2.2. The dopant in the n-region provides mobile negative charge carriers known as electrons, and the dopant in the p-region provides mobile positive charge carriers referred to as holes. When a forward voltage is applied to the p-n junction from the p- to the n-region, the charge carriers are injected across the junction into a zone where they recombine and convert their excess energy into light. The typical operating range for an LED is approximately 10–30 mA and 1.5–3 V.

When free electrons move across the p-n junction, they fall into empty holes in the p-type layer, drop from the conduction band to a lower orbit around atoms, and release energy in the form of photons. Although this phenomenon occurs in any diode, photons can be released at predefined wavelengths only when the diode consists of certain material. Otherwise, the photon's frequency is in the infrared portion of the light spectrum and becomes invisible to the human eye.

To obtain visible light, the LED material needs to provide a wide gap between the conduction and the lower orbital bands. The size of this gap determines the frequency of the photon, which in turn defines the color of the light. With the evolution of LED technology, manufacturers began to use various different materials for the semiconductor to generate peak spectral wavelengths that are associated with infrared and visible light (Held, 2016).

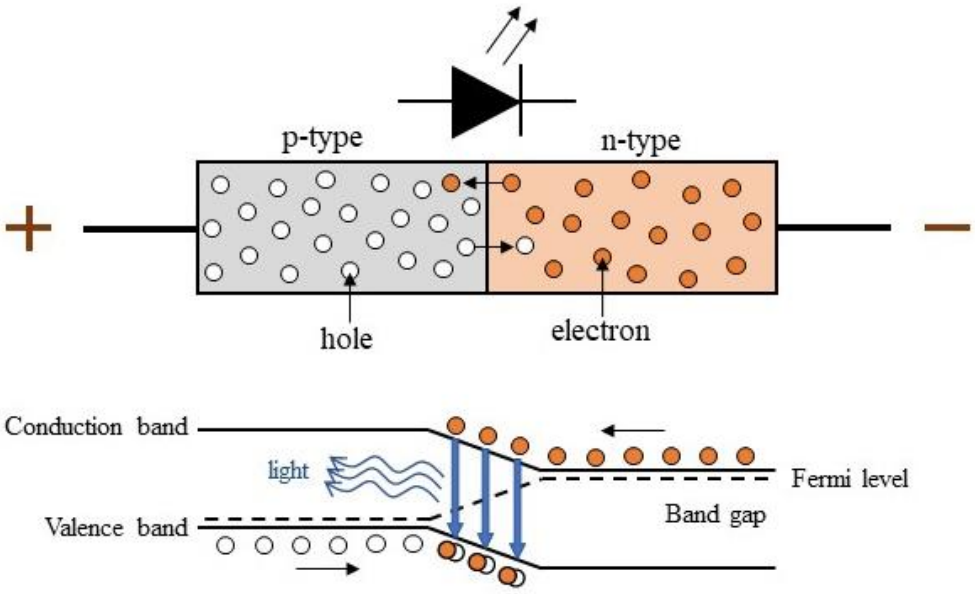

Figure 2.1 Schematics of p-n junction for LED

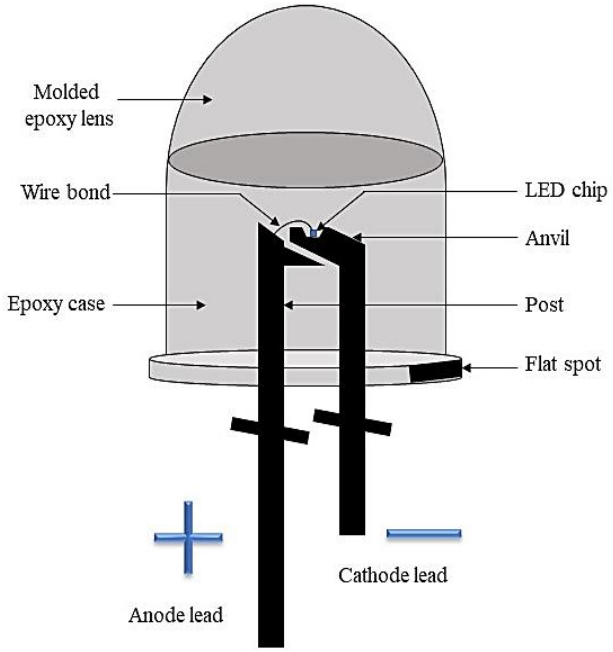

Figure 2.2 Main parts of conventional LED

2.3 White Organic LEDs

Organic electroluminescence using small molecule was first reported by Pope et al. in 1963 (Pope, Kallmann, & Magnante, 1963). The invention of efficient organic electroluminescent diodes based on heterojunction structure by Tang et al. (Tang & VanSlyke, 1987) has initiated tremendous strides of research and development for efficient and long lifetime OLEDs. In 1996, the first white LED (WLED) was developed and pioneered by Shuji Nakamura and Gerhard Fasol. This LED combines blue emission with a down-converting phosphor layer (Khanna, 2014). WLED can be fabricated in several ways, but the following are the two main processes to generate white organic light with LEDs:

1. One or more semiconducting organic thin films are sandwiched between two electrodes (Hughes & Bryce, 2005). The classic structure shown in Fig. 2.3 consists of a hole-transporting layer (HTL), electron-transporting layer (ETL), and emissive layer (EML). One electrode, such as gold (Au) or indium tin oxide (ITO), is chosen for the injection of positive charges (holes). The other electrode, such as aluminum (Al), calcium (Ca), or magnesium (Mg), is chosen for the injection of negatively charged electrons.

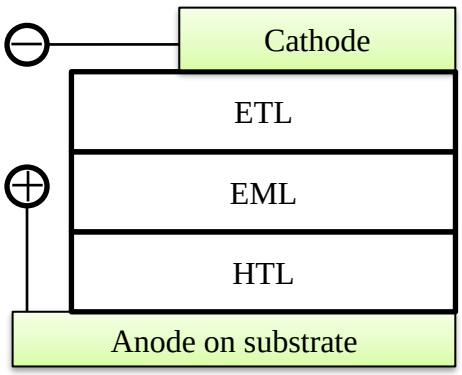

Figure 2.3 Classic heterjunction OLED structure

2. The blue light (shorter wavelength) emitted by InGaN LED is down converted in frequency (longer in wavelength) to produce yellow light with the help of a phosphor material. The combination of down-converted yellow light with low frequency and original blue light results in a white color shown in Fig. 2.4. The difference in energies between the incoming and outgoing photon beams from the phosphor represents an energy loss known as the Stokes loss, which is caused by the Stokes shift in their frequencies or wavelengths and is the principal loss component in phosphor conversion methods. Commercially, this technique is still the most important money-making means to realize white light (Khanna, 2014). UV LED can be used instead of blue LED but is often employed in combination with a red-, green-, or blue-emitting phosphor (Bruckbauer et al., 2016).

Another approach to produce white light is to synthesize or mix in the correct proportions of the emissions from separate LEDs to obtain the three complementary colors: red, green, and blue. However, this method requiring three LEDs is expensive and is therefore avoided (Khanna, 2014).

In the late 2000s, the power efficiencies of white OLEDs have overwhelmed those of incandescent bulb (~15 lm W^{-1}) by harvesting phosphorescence from OLEDs (D'Andrade & Forrest, 2004). The power efficiencies of white OLEDs (164 lm W^{-1} at 1000 cd m^{-2}) (Huang, Wu, & Fung, 2019) with light extraction are even higher than those of fluorescent lamps (70–80 lm W^{-1}). To date, white OLEDs are one of major options for ultimate white illumination source.

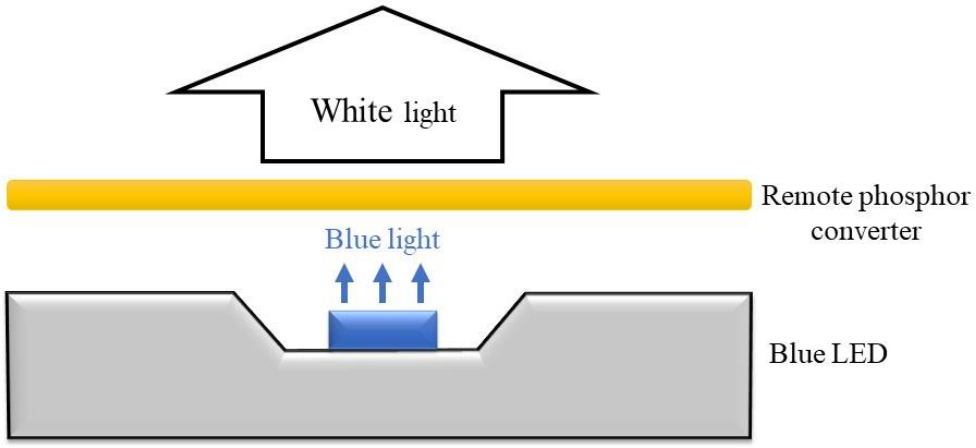

Figure 2.4 Main steps of the production of white light using remote phosphor

2.4 Concepts of light down-conversion

An inorganic–organic emitter usually consists of a UV/blue LED as the electrically generated light source and a top layer of organic materials to produce secondary (long wavelength) luminescence by down-conversion. The top layer can have several different organic materials to separately generate red, green, and blue emissions and achieve overall white light emission. Alternatively, the top organic layer and bottom LED layer can generate light with two complementary colors (yellow and blue), respectively, to obtain white light emission.

A blue-emitting GaN-based LED is used in this system as the blue light emitter. GaN has been widely known as an interesting III–V semiconductor in early 1972 (Pankove, Miller, & Berkeyheiser, 1972). Since then, GaN-based LED has been developed as highly efficient blue and green emitters. Energy transfer, such as radiative transfer between inorganic and organic counterparts, is needed to achieve the luminescence down-conversion in the layer of organic yellow-emitting material. This step requires the absorption spectra of the organic material to overlap with the emission spectra of the GaN-based LED. RE-doped metal oxide materials manufactured by high-

temperature reactions are traditionally used for down-conversion (Nishiura, Tanabe, Fujioka, & Fujimoto, 2011). The major advantage of organic materials over these phosphors is their simple processing directly from their solutions. Organic dyes, which can also be used as down-conversion materials, are also easy to process (Guha, Haight, Bojarczuk, & Kisker, 1997).

2.5 Organic dyes

Several of organic dyes, such as Lumogen® (commercialized by BASF) (Mosca et al., 2013), 4,4-difluoro-4-borata-3*a*-azonia-4*a*-aza-*s*-indacene hereafter referred to as BODIPY (Findlay et al., 2014), poly[2-methoxy-5-(2′-ethyl-hexyloxy)1,4-phenylene-vinylene] (MEH-PPV) (Sajjad et al., 2015), and 2,1,3-benzothiadiazole (BT) with fluorene and triphenylamine (TPA-Flu)2BT (Taylor-Shaw et al., 2016) are used in down-conversion LEDs as summarized in Table 2.2. Despite the abundance of fluorescent pigment-rich natural plants such as Curcuma, studies on the use of dyes extracted from nature are lacking due to certain technical and sustainability issues involved in the production and application of these dyes such as nonavailability in ready-to-use standard form, unsuitability for machine use, and limited and nonreproducible shades (Ali, Nisar, & Hussain, 2007; Saxena & Raja, 2014). One study used two vegetable extracts, namely, red Pomegranate and Curcuma extract to generate white light (V. Singh & Mishra, 2015). In 2016, another study employed curcumin to analyze the luminescence of curcumin phosphor for bio hybrid (bio-HLEDs) (Reddy & Park, 2016). The present work is the only novel innovation that used Curcuma dye for white light production.

Table 2.2 Organic dyes used in down-conversion

No	Materials	CIE (x ; y)	pumping wavelength	Light color	Ref.
1	Lumogen® F Yellow 083, a perylene-based polymer dye commercialized by BASF, and adding a small quantity of another perylene-based dye, Lumogen® F Red 305 (BASF)	(0,381 ; 0,369)	395nm, 450nm, and 490nm	warm white LEDs by yellow and red conversion	(Mosca et al., 2013)
2	[BODFluTh]2FB	(0.34, 0.31)	450nm	cold/ cool white light.	(Findlay et al., 2014)
3	poly[2,5-bis(2′,5′-bis(2″-ethylhexyloxy) phenyl)-p-phenylenevinylene] (BBEHP-PPV) and orange-red emitting poly[2-methoxy-5-(2′-ethyl-hexyloxy)- 1,4-phenylene-vinylene] (MEH-PPV)	(0.4, 0.51)	450 and 500nm	white light	(Sajjad et al., 2015)
4	(TPA-Flu)2BT and (TPA-Flu)2BTBT	not mention	444nm	white light	(Taylor-Shaw et al., 2016)
5	Red pomegranate seeds and curcuma	(0.35, 0.33) in solution, (0.26, 0.33) in gelatin gel and (0.33, 0.25) in PVA film.	380nm	white light	(V. Singh & Mishra, 2015)
6	DNA-curcumin	not mention	450nm	greenish	(Reddy & Park, 2016)

2.5.1 Band gap of organic materials

HOMO refers to the highest occupied molecular orbital, and LUMO is the lowest unoccupied molecular orbital. The difference in energy between these two levels is called a bandgap, which serves as a measurement of molecular excitability. The two

frontier bands have different terms: the upper band is called the conduction band, and the lower band is referred to as the valence band (Fleming, 2011). These bands determine the way the molecule reacts with other species. The design and fabrication of OLED devices depend on the HOMO and LUMO of organic compounds. During the formation of dimer or an aggregate of a molecule, the splitting of HOMO and LUMO is induced because of the closeness degree of the orbitals of molecules. In this process, a number of vibrational sublevels equal to the energy levels of the molecules are formed. These levels somewhat differ from each other. The number of sublevels formed depends on the number of molecules that received an impact.

When a large number of interchangeable impacts occur between the molecules, many sublevels are generated and form a continuum that is perceived as energy bands (Virk, 2014). An illustration of the gap of HOMO and LUMO is shown in Fig 2.5 (Bredas, 2014).

Orbital states can be described with terms such as filled, empty, occupied, and unoccupied. An orbital that contains the maximum number of electrons it can hold is filled, an orbital that contains no electrons is empty, and an orbital that contains at least one electron is occupied while an orbital that contains at least one open space for an electron is unoccupied. A filled orbital is occupied, but an occupied orbital is not necessarily filled. Also, an orbital can be both occupied and unoccupied, i.e., occupied means that one space is occupied by an electron and unoccupied means at least one space is free to accept an electron (Kalyani, Swart, & Dhoble, 2017).

The energy of the electrons occupying the orbits specifies the energy of the molecular structure. A π-type orbit filled matches the HOMO, and an empty π^*-type or σ^* matches the LUMO orbit.

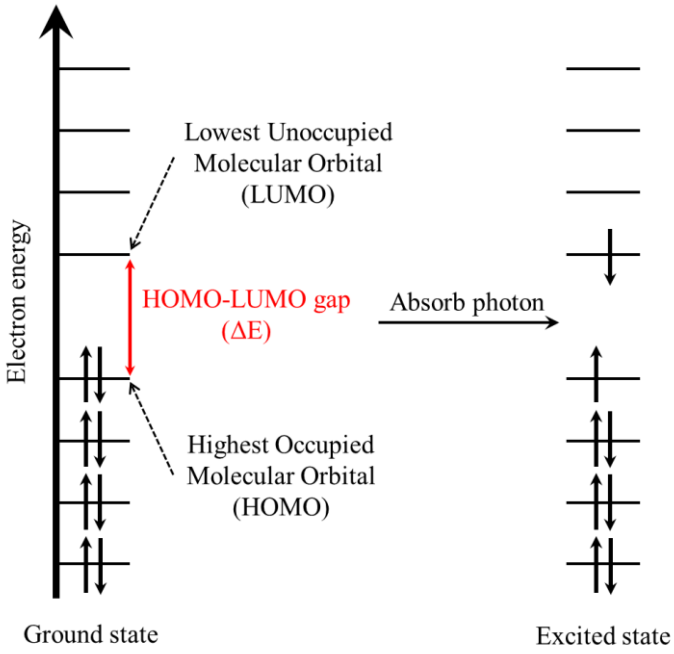

Figure 2.5 Formation of HOMO and LUMO gap (Bredas, 2014).

2.5.2 Electronic Excitation in Organic Molecules

When an atom or molecule of the sample are exposed to light having an energy that matches a possible electronic transition within the molecule, some light energy is absorbed by the electron and it jumps to a higher energy orbital. An atom can rotate and vibrate, and these two actions have distinct energy levels. Chromophores with valence electrons (with low excitation energy) control the absorption of visible light or even UV light. The spectrum with chromophores is considered complex when the transition of electrons is controlled by the rotational and vibrational transitions; the superposition produces an overlapping lines of these two transitions and therefore looks similarly to one absorption band as a result of the overlapping (Thejokalyani & Dhoble, 2014).

2.5.3 Types of absorbing electrons

The electrons that participate in the formation of bonds between atoms and those unshared outer ones (e.g., oxygen, nitrogen, and halogens) contribute to the molecules' absorption. In a single bond, the orbits are called sigma orbits that have associated sigma electrons. Meanwhile, a double bond has two molecular orbits with their associated electrons, sigma (σ) and pi (π). A parallel overlap of atomic p orbitals forms the π molecule orbital. In addition to these two types of electrons, many compounds possess unshared and nonbonding electrons referred to as the symbol n. Orbits have different energy levels; the energy level of an orbit with a nonbonding electron resides between the energy levels of π^* and σ^* orbital (i.e. the anti-bounding) and the bonding energy levels. Radiation absorption causes an electronic transition according to a specific energy level (Thejokalyani & Dhoble, 2014). Electronic excitation in organic molecules is illustrated in Fig. 2.6. Transitions $n \rightarrow \pi^*$ correspond to excitation of an electron of an unshared pair to an antibonding orbital (π^*). This transition involves least amount of energy than all the transitions and therefore, this transition gives rise to an absorption band at longer wavelengths. Transitions $\pi \rightarrow \pi^*$ correspond to excitation of an electron from a bonding orbital (π) to an antibonding (π^*). Transitions $n \rightarrow \sigma^*$ correspond to excitation of an electron of an unshared pair to an antibonding orbital (σ^*) of a σ bond. Transitions $\pi \rightarrow \sigma^*$ correspond to excitation of an electron from a bonding orbital (π) to a higher energy antibonding orbital of the single bond, σ^* (sigma star). Transitions $\sigma \rightarrow \pi^*$ correspond to excitation of a σ electron of a single bond to an antibonding orbital (π^*). Transitions $\sigma \rightarrow \sigma^*$ correspond to excitation of a σ electron of a single bond to a higher energy antibonding orbital of the single bond, σ^* (sigma star). The

energy required is large. Absorption maxima due to σ → σ* transitions cannot be viewed in typical UV-Visible spectra (Roberts & Caserio, 1977; Sharma, 2007).

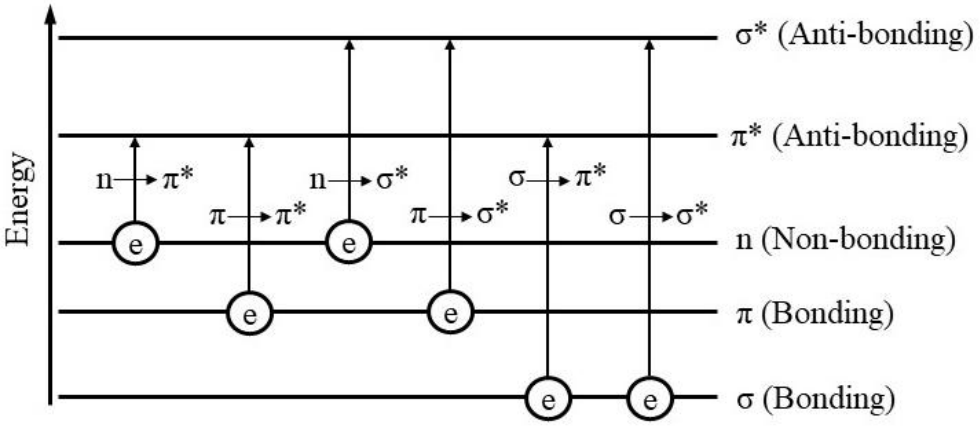

Figure 2.6 Various electronic excitations that occur in organic molecules (Thejokalyani & Dhoble, 2014).

Among the six transitions outlined, only the two lowest energy ones (n→π* and π→π*) can be done by the energies available in the 200 nm (in the near ultra-violet) to 800 nm (in the very near infra-red) spectrum. The relationship between the energy and frequency of light absorbed is as follows:

$$E=hv, \tag{2.1}$$

where E is the energy of light, h is planck's constant, and v is frequency of light. The relationship between wavelength and frequency is as follows:

$$v = \frac{c}{\lambda} \tag{2.2}$$

where λ is the wavelength, c is the speed of light, and v is frequency. 2.2 equation indicates that the wavelength is short when the frequency is high. If high energy jump is supplied, light will be absorbed at a high frequency, i.e. at a short wavelength.

Fig. 2.7 shows an example of the simple absorption spectrum for molecules. Absorbance (on the vertical axis) is the amount of light absorbed in percentage. When

its value is high, much of the particular wavelength is being absorbed. The absorption peaks at a value of 222 nm, which is located in the UV spectrum. Hence, the absorbed light is in the invisible light range. The figure indicates a broad absorption peak rather than a single line at 222 nm. A jump from a π bonding orbital to a π anti bonding orbital must have fixed energy and therefore absorbs a fixed wavelength. This problem arises because rotations and vibrations in the molecules continually change the energies of the orbitals and the gaps between them. As a result, absorption transpires over a range of wavelengths rather than at one fixed one. As a rule, the energetically favored electron promotion occurs from HOMO to LUMO, and the resulting species is called an excited state (Sagadevan & Murugasen, 2014).

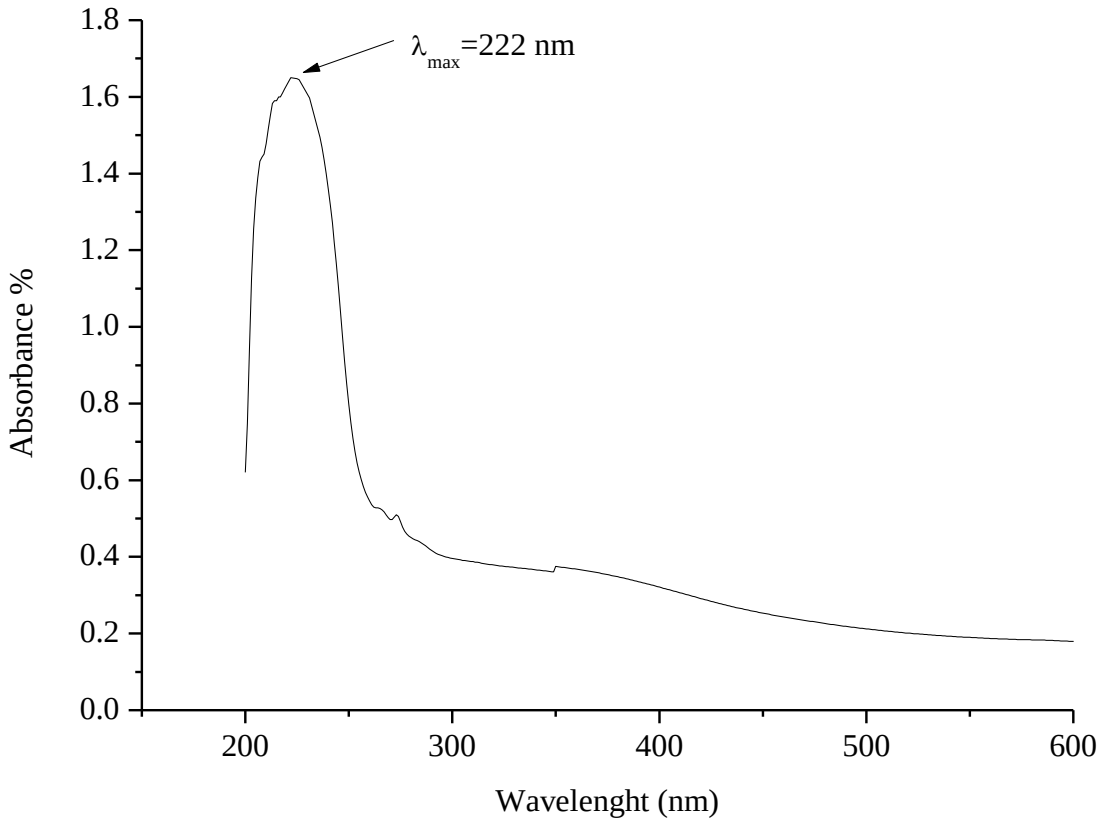

Figure 2.7 Simple absorption spectrum for molecules.

The n or π electron transition to the π* excited state can be observed in many absorption spectroscopies in organic compounds because this process happens in the visible electromagnetic spectrum area and requires the unsaturated group to provide the π electrons. Molar absorptions from n→π* transitions range between 10 and 100 L mol^{-1} cm^{-1}, and those from π→π* transitions range between 1000 and 10,000 L mol^{-1} cm^{-1}. The absorbing species dissolved in the solvent affects the spectrum of the species. When increasing the solvent polarity that lowers the energy of the n orbital, the transition forming n→π* with peaks shifts to blue shifts with short wavelengths. In other words, the attractive polarization forces of the solvent and absorber decrease the energy levels for the excited and unexcited states, with the effect higher for the excited state than for the unexcited state. Therefore, the energy difference between the two states is minimally reduced, thereby causing an extremely small red shift and effect the transition π→π*. On the contrary, the solvation of lone pairs causes a blue shift that consequently overshadows the effect of the transition from *n* to π* (Thejokalyani & Dhoble, 2014).

2.5.4 Tauc method for optical absorption edge determination

Tauc et al. (Tauc, Grigorovici, & Vancu, 1966) investigated the optical and electronic properties of amorphous germanium and proposed and substantiated a method for determining the bandgap by plotting optical absorbance data versus energy. This technique was further developed in Davis and Mott's general work on amorphous semiconductors (Davis & Mott, 1970). They showed that the optical absorption strength depends on the difference between the photon energy and the bandgap as follows:

$$(\alpha h\nu)^{1/n}=A(h\nu-E_g) \quad (2.3)$$

where h is Planck's constant, ν is the photon's frequency, α is the absorption coefficient, n is the nature of the electronic transition, E_g is the bandgap, and A is a proportionality

constant. The value of the exponent denotes the nature of the electronic transition, whether allowed or forbidden and whether direct or indirect:

for direct allowed transitions: n =1/2,

for direct forbidden transitions: n = 3/2,

for indirect allowed transitions: n = 2,

for indirect forbidden transitions: n = 3.

In general, the allowed transitions dominate the basic absorption processes, with either n= 1/2 or n = 2 for direct or indirect transition, respectively (Viezbicke, Patel, Davis, & Birnie III, 2015).

Thus, the basic procedure for a Tauc analysis is to acquire optical absorbance data within a range of energy from below to above the bandgap transition. Plotting the $(\alpha hv)^{1/n}$ versus (hv) can be applied for testing n =1/2 or n =2 to distinguish which of them provides the better fit and thus identify the correct transition type (Viezbicke et al., 2015).

To find the value of *Eg*, we need to determine the relationship between *Eg* and $(\alpha hv)^{1/n}$ then find the point of intersection of the tangent ray with the X axis. The following equation can be used to determine the values of the X axis (*Eg*):

$$Eg = \frac{1240}{\lambda} \tag{2.4}$$

The following equation can be used to determine the values of the Y-axis, $(\alpha hv)^{1/n}$:

$$(\alpha hv)^{1/n} = (2.303 \; x \; A \; x \; Eg), \tag{2.5}$$

where *A* is the absorbance in percentage.

Fig.2.8 gives one example of a Tauc plot for Gamal (*Gliricidia Sepium*) leaves extract (Johannes, Pingak, & Bukit, 2020). The characteristic features of Tauc plots are evident: at low photon energies, the absorption approaches zero, and the material is transparent. When near the bandgap value, the absorption intensifies and shows a region

of linearity in this squared exponent plot. This linear region is used to extrapolate to the X axis intercept to find the bandgap value (approximately 1.83 eV). At extremely high energies, the absorption processes saturate, and the curve deviates again from the linear trend.

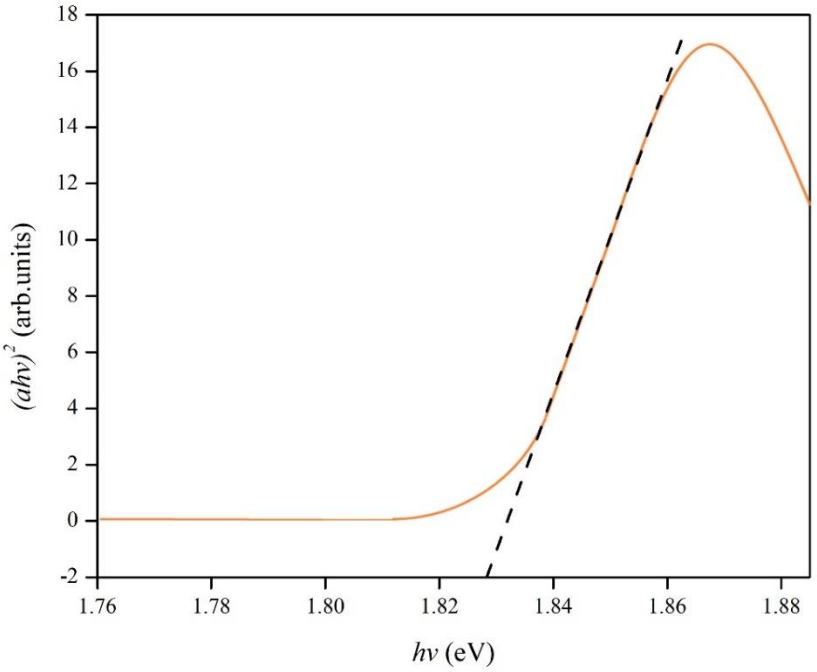

Figure 2.8 Example Tauc plot from the UV-vis analysis of Gamal (*Gliricidia Sepium*) leaves extract, that illustrates the method of fitting the linear region to evaluate the bandgap at the X axis intercept (approximately 1.83 eV) (Johannes et al., 2020).

2.6 Turmeric (Curcuma longa L.)

Curcuma longa L. is composed of carbohydrates, proteins, amino acids, alkaloids, terpenoids, and flavonoids (Pawar, Karde, Mundle, Jadhav, & Mehra, 2014). The main components extracted from curcuma are curcuminoids, particularly CUR, DMC, and BDMC (Hatamipour et al., 2019; Itaya et al., 2019). CUR is the major component responsible for the yellow color of curcuma (Priyadarsini, 2014). Its color varies depending on the protein concentration. CUR has many double bonds connecting the aromatic rings on the ends of the molecules; hence, the energy levels are close to